Progress in NUCLEAR SCIENCE and TECHNOLOGY, Vol. 2, pp.568-575 (2011)

**ARTICLE**

# Evaluation of the Effects of Gamma Irradiation from a $^{9}$Be Neutron Source in Digital ASIC's with GEANT4

Miguel A. CORTÉS-GIRALDO[1,*], Francisco R. PALOMO[2], Esther GARCÍA-SÁNCHEZ[2] and José M. QUESADA[1]

[1]*Departamento de Física Atómica, Molecular y Nuclear, University of Sevilla, 41080-Sevilla, Spain*
[2] *Departamento de Ingeniería Electrónica, Escuela Superior de Ingenieros, University of Sevilla, 41092-Sevilla, Spain*

This work presents a GEANT4 application (version 9.3.p01) for the calculation of gamma/neutron dose on a AMISC5 flip-flop target from a proton/deuteron $^{9}$Be neutron source. For comparison purposes, a gamma irradiation campaign using a $^{60}$Co standard irradiation source was also simulated. In all cases we consider energy rate per unit volume for comparison in future experiments in order to establish differences between radiation effects on electronics due to neutron/gamma and pure gamma beams.

***KEYWORDS: GEANT4, ASIC, VLSI, microdosimetry, neutrons, gammas***

## I. Introduction

This work presents Monte Carlo simulations with the GEANT4 toolkit[1)] (version 9.3.p01) of a new neutron source facility, planned at CNA (Centro Nacional de Aceleradores, Sevilla, Spain),[2)] with the purpose of arranging a suitable setup. GEANT4 has been used recently for neutron production analysis of a high energy spallation source.[3)] In this work we concentrate on a low energy neutron source. A cyclotron from IBA[4)] will produce an 18 MeV proton beam (current of up to 100 $\mu$A) and a 9 MeV deuteron beam (current of up to 40 $\mu$A) focused on a $^{9}$Be target. The charged particles will impinge on a 5-mm-thick $^{9}$Be slab, placed at the back of a refrigeration drum, creating a secondary neutron beam used for the irradiation of CMOS microelectronics circuits.

Fast neutron effects on microelectronics is a growing field due to concerns related to atmospheric neutron effects on high integrated microelectronics[5)] and in general for microelectronics endurance in neutron environments. For that reasons the neutron (and parasitic gammas) end target is a flip-flop, modelled from VLSI On Semiconductor C5 technology kit.[6)] In the Monte Carlo simulations, the flip-flop target has been implemented as a CAD model using the FASTRAD tool[7)] and imported to GEANT4 by means of the GDML[8)] interface.

The expected output will be a neutron beam plus parasitic gamma photons. That parasitic gammas are emmited from the $^{9}$Be target, by means of $^{9}$Be(p,n$\gamma$)$^{9}$B for proton beam, and by means of $^{9}$Be(d,n$\gamma$)$^{10}$B and $^{9}$Be(d,p$\gamma$)$^{10}$Be for deuteron beam. Fast neutron production by stripping/break-up reactions induced by deuteron/proton beams on a $^{9}$Be thick target is a well-known method.[9,10)] CMOS transistors are more vulnerable to radiation damages produced by gammas than those produced by neutrons.[11)] Therefore, it is important to obtain a low gamma to neutron ratio by selecting the appropriate nuclear reaction. We calculate the neutron/gamma ratio for the beams considered using the GEANT4 toolkit. The contribution of the parasitic gamma irradiation will be compared with experimental measurements with a Co-60 irradiator, supplied by J. L. Shepperd & Assoc. (model 484C), that is planned for installation at CNA.

The GEANT4 Monte Carlo simulations are devoted to calculate the energy deposited per unit volume and event in three types of sensitive volumes in the flip-flop: transistor gate oxides, field oxides and transistor channels.[11)] From the literature it is known that oxides can acumulate charge generated by ionization[12)] (Total Ionization Dose –TID– effects, esentially from the gamma rays interaction and minor contribution from the neutron interaction) and the channels are sensitive to Non-Ionizing Energy Loss (NIEL) by neutrons due to linear momentum transfer.[13)]

With regard to the neutron and gamma production, GEANT4, as the other current Monte Carlo codes, such as MCNPX or PHITS, when applied for proton and deuteron transport calculations use built-in models to describe nuclear interactions. These models are found unreliable in predicting neutrons and photons generated by low energy protons and deuterons. In order to overcome this problem, secondary neutron beams from proton/deuteron $^{9}$Be source have been generated following the experimental thick target data published by Brede *et al.*[14)] However, the production of gammas in the $^{9}$Be source has been simulated with the GEANT4 toolkit due to the abscence, to our knowledge, of experimental data.

In Section II we describe the GEANT4 model of the neutron source, which uses the proton and deuteron beams produced by the IBA cyclotron. The Monte Carlo calculations of the emission spectra from the source are presented in Section III. Section IV is devoted to describe the flip-flop circuit, ir-

*Corresponding author, E-mail: miancortes@us.es

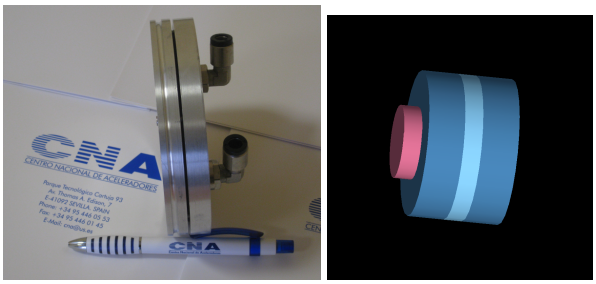


**Fig. 1** Left: a picture of the refrigeration drum. Right: $^{9}$Be slab (reddish volume) and refrigeration drum (layers from left to right: steel, water and steel) geometry model. The beam enters from the left side and passes the $^{9}$Be slab (thickness of 5 mm) and the refrigeration drum (thickness of 1 cm for the steel layers and of 5 mm for the water layer).

radiated by the secondary emission produced by the neutron source. Section V presents the calculations of the energy deposition, per unit volume and event, by neutrons and parasitic gammas emitted by the neutron source in key elements of the flip-flop. For comparison purposes, in Section VI we show the results obtained for the flip-flop irradiated with a Co-60 source. The conclusions are presented in Section VII.

## II. GEANT4 Model of the Neutron Source

**Figure 1** presents a photograph of the refrigeration drum and the geometric model of the beryllium slab and the refrigeration drum made for the GEANT4 simulations. The primary beam (coming out of the cyclotron) enters from the left in Fig. 1. After the beryllium slab (thickness of 5 mm), the beam passes through the refrigeration drum, composed of three layers made of, in this order, steel (1 cm), water (5 mm) and steel (1 cm). The transversal dimensions are not relevant for the studies presented in this work, since, due to the extremely small solid angle subtended by the flip-flop (see Section V), the emission of secondaries is only analysed at 0$^{o}$.

Neutron transportation is deeply rooted in Monte Carlo method, since it was its first application.[15] Recent works have demonstrated the capability of GEANT4, general purpose radiation transport toolkit, for such calculations.[16,17] Nevertheless, with regard to neutron production, nuclear models describing the responsible mechanisms at typical neutron source energies are not implemented in a realistic manner in any of the present-day transport codes. This situation is circumvented in some cases by assuming monoenergetic neutron beams at the energies where neutron production cross sections are peaked.[18] In other cases, in order to get realistic initial neutron spectra to be transported, dedicated channel-specific nuclear reaction codes (accessing to evaluated data) are used.[17,19] In any case, the description of the initial neutron source spectrum forces to resort either to extremely simplifying assumptions or to external calculations.

The emission of secondary neutrons and gammas in the beryllium slab, to be used as primay particles in GEANT4, was simulated according to the experimental thick target data published by Brede *et al.*[14] In that work, the beam energy ranged from 9.43 MeV to 13.54 MeV for deuterons and from 17.24 MeV to 22.01 MeV for protons. The energy spectrum of the neutrons emitted with a proton beam at 18 MeV was calculated considering a linear interpolation between the experimental values at 17.24 MeV and 18.16 MeV. The energy distribution of the neutrons emitted with a deuteron beam at 9 MeV was estimated with a linear extrapolation of the three lowest energies experimentaly measured in the referred work,[14] 9.43 MeV, 10.06 MeV and 10.68 MeV. The shape of the published spectrum was taken into account where linear extrapolation could not provide reliable results.

The emission of secondary gammas in the $^{9}$Be slab was directly simulated with GEANT4, since to our knowledge there are no experimental data of gamma emission in these conditions. After the simulation of the proton and deuteron bombardment of the production target, gammas produced at forward angles were stored in a phase-space file in IAEA format using the code developed by our group for reading/writing IAEA phase-space files with GEANT4 (available online),[20] since only gammas in a extremely small solid angle around 0$^{o}$ will reach the flip-flop, placed at 1 m distance.

The secondary neutrons and gamma emitted in the $^{9}$Be slab were used as the primary particles of a GEANT4 application which simulates the transport of particles through the refrigeration drum. The *Primary Generator Action* class coded in this application is capable of

- reading an ASCII file containing the previously obtained neutron energy spectra from a proton (18 MeV) or deuteron (9 MeV) beam on the 5-mm-thick $^{9}$Be slab, in order to generate the energy distributions of the primary neutrons at 0$^{o}$ according to them.
- reading the gammas stored in the IAEA phase-space file previously mentioned by making use of the code developed by our group.[20]

The transport of particles through the whole experimental setup was simulated with GEANT4 using *Livermore Low-Energy*[21,22] and *QGSP_BIC_HP*[23] physics list. Electromagnetic interactions were simulated with the GEANT4 *Livermore Low-Energy Electromagnetic (EM)* package, which extends its application range down to 250 eV. Rayleigh scattering and atomic relaxation processes are implemented in this package. These models implement cross-section tables obtained from the Lawrence Livermore National Library, including evaluated data for photons,[24] electrons[25] and atoms.[26] Since no data for positrons are present, GEANT4 *Standard EM* physics list[27] is used in this case. Production cut value was set to 500 nm, which means that all the secondary electrons, gammas and positrons with initial kinetic energy above 250 eV are tracked. In addition, as an internal safety check, GEANT4 can produce secondaries below this threshold when the distance between the point where the secondary particle is created and any geometric boundary is less than the production cut value.[28] Hadronic interactions were modelled with the *QGSP_BIC_HP* physics list, which uses the Binary cascade model implemented in GEANT4 for the transport of protons, neutrons and ions with energies below $\sim$10 GeV. For neutrons below 20 MeV, which corresponds to the energy

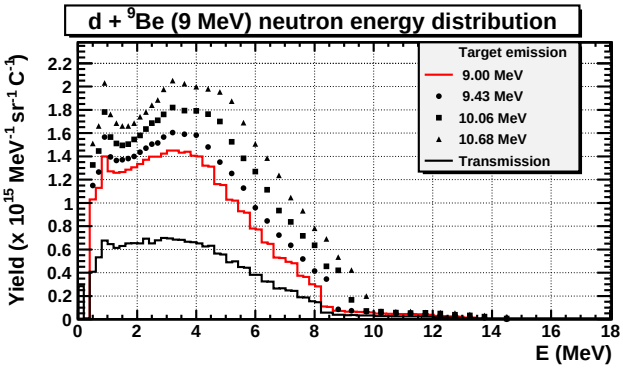


**Fig. 2** Energy distribution of the neutrons emitted at 0° by means of $^{9}$Be(d,n$\gamma$)$^{10}$B reaction with a deuteron beam at 9 MeV. The red histogram shows the neutron emission in the beryllium slab. The black histogram plots the neutron yield coming out of the source after passing through the refrigeration drum. The values published by Brede *et al.*[14] used to estimate the emission in the $^{9}$Be slab are also plotted.

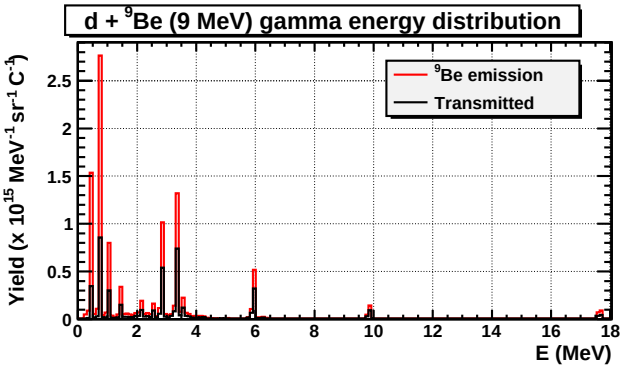


**Fig. 3** Energy distribution of the gammas emitted at 0° by means of $^{9}$Be(d,p$\gamma$)$^{10}$Be and $^{9}$Be(d,n$\gamma$)$^{10}$B reactions with a deuteron beam at 9 MeV. Histogram representation follows the same criteria as in Fig. 2.

range covered in this work, the *high precision* (HP) package (which uses G4ENDL data library, mainly based on ENDF/B,[29] JEFF[30] and JENDL[31] evaluated nuclear data) is used instead.

## III. Simulation of Particle Emissions

According to the previous section, to evaluate the production of secondaries in the neutron source with GEANT4, the transport of neutrons and gammas produced in the $^{9}$Be slab under the irradiation of a proton (deuteron) beam through the refrigeration drum model (Fig. 1) was simulated. Apart from the characterization of the energy spectra, we were also interested in the estimation of the production ratio of neutrons over gammas in order to decide the most suitable setup for neutron emission.

**Figure 2** shows the spectral yield at 0° of the neutrons produced in the $^{9}$Be slab with a deuteron beam at 9 MeV

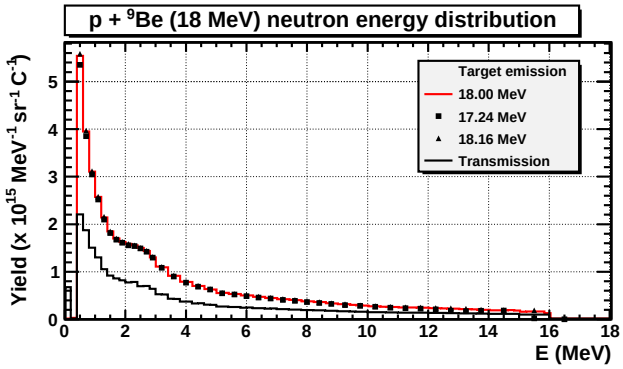


**Fig. 4** Energy distribution of the neutrons emitted at 0° by means of $^{9}$Be(p,n$\gamma$)$^{9}$B reaction with a proton beam at 18 MeV. Histogram representation follows the same criteria as in Fig. 2. The values published by Brede *et al.*[14] used to estimate the emission in the $^{9}$Be slab are also plotted.

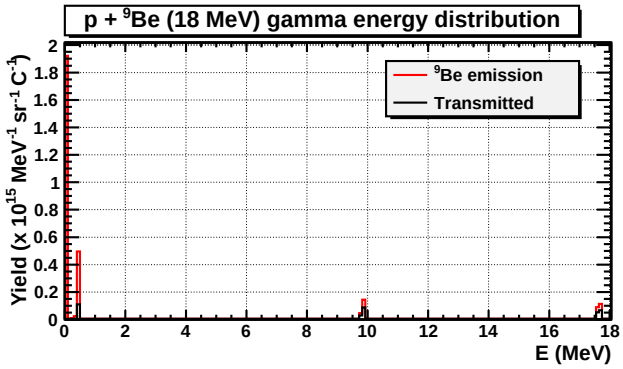


**Fig. 5** Energy distribution of the gammas emitted at 0° by means of $^{9}$Be(p,n$\gamma$)$^{9}$B reaction with a proton beam at 18 MeV. Histogram representation follows the same criteria as in Fig. 2.

(red histogram) compared with the experimental yields published by Brede *et al.*[14] The spectral yield of neutrons transmitted through the refrigeration drum of the source, calculated with GEANT4, is also presented in Fig. 2 (black histogram). The transmission ratio, calculated as the fraction of neutrons reaching a circle of radius 1 cm placed at a distance of 1 m after passing through the drum, was $(50 \pm 1)$%. The integral yield of neutrons in the $^{9}$Be slab corresponds to $(8.4 \pm 0.8) \times 10^{15}$ sr$^{-1}$ C$^{-1}$. This value was calculated using our extrapolated data and the uncertainty was 10%, which corresponds to the largest uncertainty discussed by Brede *et al.*[14] Then, the calculated integral yield of neutrons emmited from the source (after passing through the refrigeration drum) at 0° was $(4.1 \pm 0.4) \times 10^{15}$ sr$^{-1}$ C$^{-1}$.

**Figure 3** presents the spectral yield of the parasitic emission of gammas from the neutron source with a deuteron beam 9 MeV. In this case no experimental data were found and, therefore, the emission spectrum was produced with GEANT4. As expected, the transmission ratio through the refrigeration drum becomes higher for higher energies. In av-

erage terms, the transmission ratio was $(45 \pm 1)\%$. It must be noted that the secondary emission of gammas in the refrigeration drum due to the interaction of neutrons was also studied, but the contribution of these secondary gammas to the total flux at 0º was three orders of magnitude lower than the actual transmission from the $^9$Be slab. The calculated yield of gammas coming out of the source at 0º was $(5.1 \pm 0.2) \times 10^{14}$ sr$^{-1}$ C$^{-1}$. This calculation was done by estimate the flux through a 5 cm radius circle placed at 1 m distance, normalized by solid angle. The uncertainty of the yield corresponds to the $1\sigma$ level of the statistical uncertainty obtained in the GEANT4 simulations.

With these values, the neutron/gamma production ratio at 0º calculated with GEANT4 was $8.0 \pm 0.8$ neutrons per gamma for a deuteron beam at 9 MeV.

**Figures 4-5** show the corresponding results for the irradiation of the $^9$Be slab with a proton beam at 18 MeV. The procedure and criteria followed were the same as with the deuteron beam at 9 MeV (Figs. 2-3). The transmission ratio of neutrons through the refrigeration drum was $(50 \pm 1)\%$. This value was expected since the energy range of the neutrons is the same as for deuterons at 9 MeV. The transmission ratio of photons was $(15 \pm 1)\%$, lower than the value calculated for deuterons since the photon spectrum is concentrated below 1 MeV. The integral yield of neutrons estimated in the $^9$Be slab with our interpolation was $(1.1 \pm 0.1) \times 10^{16}$ sr$^{-1}$ C$^{-1}$. The integral yield of neutrons transmitted through the drum at 0º was $(5.5 \pm 0.6) \times 10^{15}$ sr$^{-1}$ C$^{-1}$, whereas a yield of $(4.4 \pm 0.3) \times 10^{13}$ sr$^{-1}$ C$^{-1}$ was calculated for photons.

Thus, the neutron/gamma production ratio at 0º calculated with GEANT4 was $(1.2 \pm 0.2) \times 10^2$ neutrons per gamma for a proton beam at 18 MeV.

It must be noted that we observe in Fig. 3 and in Fig. 5 two spurious peaks at 9.8 MeV and 17.6 MeV. We investigated carefully the origin of those peaks in the Monte Carlo simulations, finding that these gammas were produced by GEANT4 from the n+$^9$Be inelastic reaction occuring in the Be slab. This reaction, simulated by *G4NeutronHPInelastic* process of the GEANT4 toolkit, was not simulated properly with the version used in this work. Nevertheless, this inelastic reaction will be fixed for future releases.[a]

In any case, the relative contribution of that spurious emission of gammas is higher with the proton beam than with the deuteron beam. Therefore, according to the GEANT4 simulations, we expect that the quality of this planned neutron source must be higher with the 18 MeV proton beam than with the 9 MeV deuteron beam. Naturally, these results must be compared with experimental data to provide final support to the Monte Carlo calculations.

## IV. Target Description

The master-slave type CMOS flip-flop schematics is shown in **Fig. 6**. For a total of 28 transistors (14 nMOS and 14 pMOS), the clock buffer has two CMOS inverter gates (4 transistors), the master stage has 4 CMOS inverter gates (14 transistors), including key transistors, and the slave stage has 4 CMOS inverter gates (10 transistors). Inverter transistors are designated with the code CX, key transistors are named as TX and the clock buffer transistors are labelled with the codes nCLK_nMOS, CLK_nMOS, CLK_pMOS and nCLK_pMOS. More details can be found elsewhere.[32)]

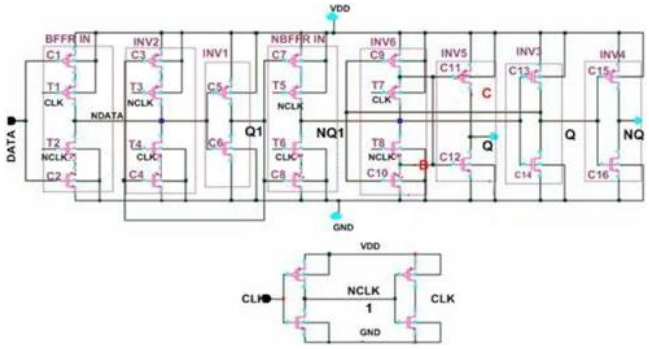


**Fig. 6** Flip-Flop schematic, it has a master-slave flip-flop architecture (upper figure), with an input clock buffer (bottom figure).

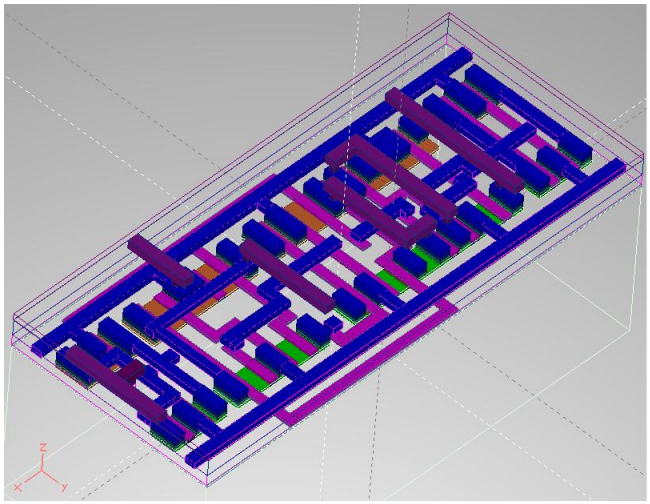

**Fig. 7** FASTRAD 3D CAD model of the master-slave flip-flop with input clock buffer, extracted from the layout design of the flip-flop. Depicted are the two aluminium layers (blue, purple), the polysilicon lines (pink) and the transistor bodies (orange for pMOS, green for nMOS).

GEANT4 can import geometry models from CAD software by means of its GDML interface.[8)] The 3D CAD model of the flip-flop geometry was made with FASTRAD,[7)] using the dimensions taken from the flip-flop layout (see **Fig. 7**). The flip-flop is part of an ASIC designed for irradiation testing at the Electronics Engineering Dpt.[33)] where two of the authors are working. The flip-flop was designed with the On Semiconductor C5 VLSI kit[b] available through the MOSIS programme.[6)] It is a three metal, two polysilicon, n-well, 0.5 micron technology, very well known in the microelectronics field because it was released around mid 90's. In our flip-flop design we use only two metal layers and one polysilicon layer.

[a] T. Koi (SLAC), private communication.

[b] formerly known as AMISC5 kit from the AMS foundry.

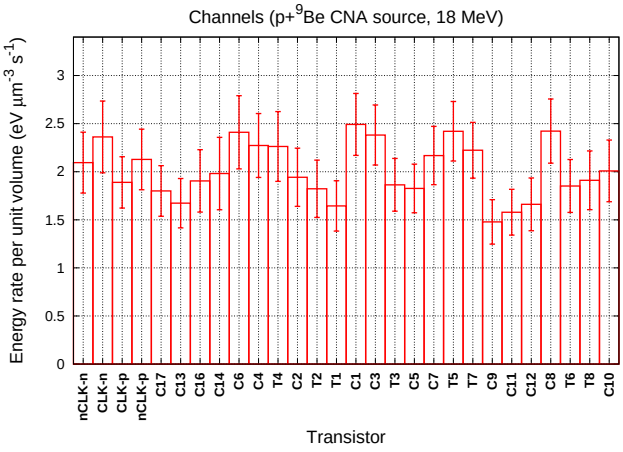


**Fig. 8** Energy deposition rate, per unit volume, in the channels of the flip-flop transistors by the neutrons emitted from the $^{9}$Be source irradiated with an 18 MeV proton beam with intensity of 100 $\mu$A. Labels in abscissa indicate the transistor. The transistor type, NMOS (-n) or PMOS (-p), is specified in case of ambiguity.

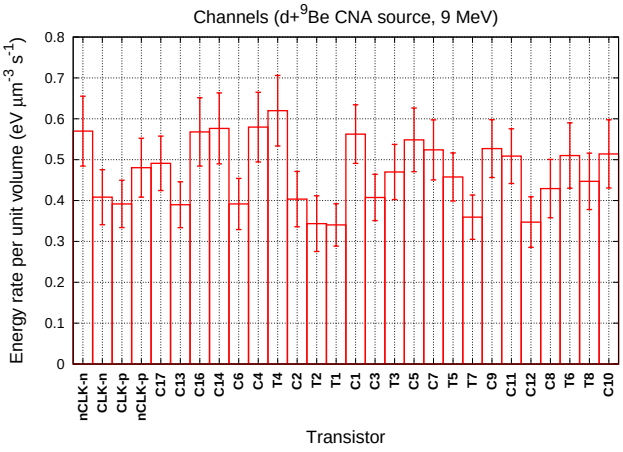


**Fig. 9** Energy deposition rate, per unit volume, in the channels of the flip-flop transistors by the neutrons emitted from the $^{9}$Be source irradiated with a 9 MeV deuteron beam with intensity of 40 $\mu$A. Labelling is the same as in Fig. 8.

The surface of the flip-flop is 24.0×55.5 $\mu$m$^2$ and is covered with a 400-nm-thick field oxide in places where there are no transistors. A pMOS transistor has an area of $(x = 4.05)\times(y = 4.0)$ $\mu$m$^2$ and a nMOS transistor has an area of $(x = 4.05)\times(y = 3.0)$ $\mu$m$^2$. As discussed in the introduction, we consider gate oxides, field oxides and channels as sensitive volumes for neutron and gamma irradiation. The gate oxide volume is $(x = 1.05)\times(y = 4.0)\times(z = 0.0125)$ $\mu$m$^3$ for a pMOS transistor and $(x = 1.05)\times(y = 3.0)\times(z = 0.0125)$ $\mu$m$^3$ for a nMOS transistor. The channel volume is $(x = 1.05)\times(y = 4.0)\times(z = 0.3)$ $\mu$m$^3$ for a pMOS transistor and $(x = 1.05)\times(y = 3.0)\times(z = 0.3)$ $\mu$m$^3$ for a nMOS transistor.

We use this GEANT4 application to calculate the energy distribution and the microdosimetry in the flip-flop target from the neutron beams. Finally, to assess the potential radiation damage produced in the flip-flop by parasitic gammas, these results are compared with a standard $^{60}$Co gamma source. The contributions to the energy deposited by neutrons and gammas was evaluated separately in order to study the most sensitive element of the flip-flop for each kind of radiation.

## V. Target Irradiation Results

Experimental energy spectra[14] were considered to simulate the production of neutrons in the $^{9}$Be target. Neutrons were generated at the end of the $^{9}$Be slab with $\theta = 0^{o}$, and propagated through the refrigeration drum. Finally, neutrons crossing a plane placed at a distance of 1 m from the target, without having any angular deviation, were recorded to generate the resulting energy spectrum at this distance, which corresponds to the position of the flip-flop. This procedure can be done due to the extremely small solid angle subtended by the flip-flop, $\Omega_{\rm ff}$, at a distance of 1 m ($\Omega_{\rm ff} = 1.33 \times 10^{-9}$ sr).

The irradiation of the flip-flop with the energy spectra of the neutrons and gammas coming out of the source (through the refrigeration drum) was simulated to evaluate the energy deposition rate per unit volume in the sensitive volumes of the flip-flop. For each situation, $3 \times 10^{9}$ events were simulated. An "event" is one particle reaching the flip-flop. The energy deposition rate per unit volume was obtained by multiplying the energy deposited per unit volume and event (calculated with Monte Carlo simulations) by the yield at $0^{o}$ (see Section III), the solid angle $\Omega_{\rm ff}$ and the beam intensity. **Figure 8** shows the energy deposition rate per unit volume in the channels by the neutrons produced when the source is irradiated with a proton beam at 18 MeV with an intensity of 100 $\mu$A. The error bars represent the statistical uncertainties, which were calculated with the method published by Walters *et al.* for dosimetry calculations.[34] The average value of the uncertainties was 15% (1 $\sigma$). Since the field oxides are present around every transistor of the flip-flop, we also calculated the average neutron dose rate in the field oxides, $d_{\rm fo,pn}$, in order to estimate the average dose rate throughout the circuit. The calculated value was

$$d_{\rm fo,pn} = (1.7 \pm 0.2) \times 10^{-4} \text{ Gy/s}.$$

The energy deposition rate per unit volume in the channels by the neutrons produced when the source is irradiated with a deuteron beam at 9 MeV with an intensity of 40 $\mu$A is represented in **Fig. 9** with statistical uncertainties (15%, 1 $\sigma$). In this case, the average neutron dose rate in the field oxides, $d_{\rm fo,dn}$ was

$$d_{\rm fo,dn} = (4.2 \pm 0.4) \times 10^{-5} \text{ Gy/s},$$

which is comparable with the dose rate calculated previously with the proton beam.

The energy deposition rate per unit volume in the gate oxides due to the parasitic gammas produced in the source with the proton beam at 18 MeV (100 $\mu$A) was also calculated to compare with the irradiation by neutrons. The results are shown in **Fig. 10**; the statistical uncertainties are between 13%

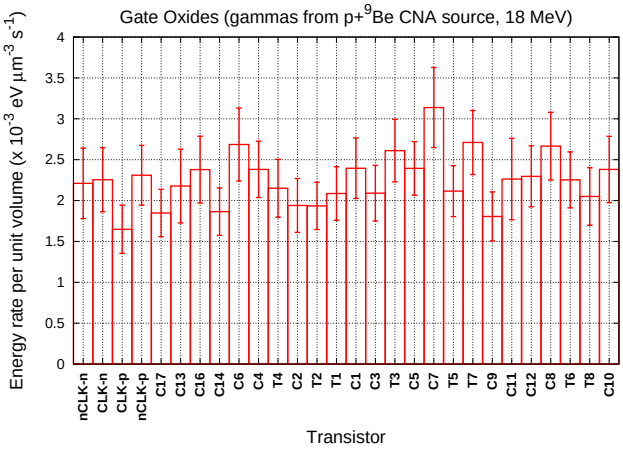


**Fig. 10** Energy deposition rate, per unit volume, in the gate oxides of the flip-flop transistors by the parasitic gammas emitted from the $^{9}$Be source irradiated with an 18 MeV proton beam with intensity of 100 $\mu$A. Labelling is the same as in Fig. 8.

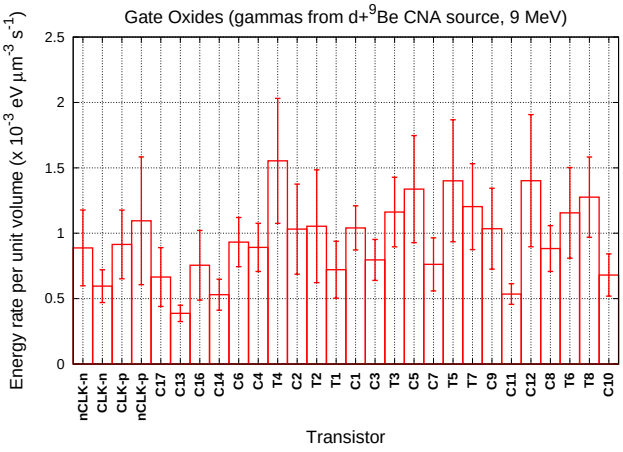


**Fig. 11** Energy deposition rate, per unit volume, in the gate oxides of the flip-flop transistors by the parasitic gammas emitted from the $^{9}$Be source irradiated with a 9 MeV deuteron beam with intensity of 40 $\mu$A. Labelling is the same as in Fig. 8.

and 22% (1 $\sigma$). The average dose rate in the field oxides due to the parasitic gamma irradiation, $d_{\mathrm{fo,p}\gamma}$, was

$$d_{\mathrm{fo,p}\gamma} = (1.4 \pm 0.1) \times 10^{-7}\ \mathrm{Gy/s},$$

which is three orders of magnitude lower than the dose rate calculated for the neutrons emitted with the proton beam, $d_{\mathrm{fo,pn}}$.

The energy deposition rate per unit volume in the gate oxides by the parasitic gammas emitted from the source, when irradiated with the deuteron beam at 9 MeV (40 $\mu$A), is plotted in **Fig. 11**; the statistical uncertainties are between 14% and 40% (1 $\sigma$). The average dose rate in the field oxides due to the parasitic gamma irradiation, $d_{\mathrm{fo,d}\gamma}$, was

$$d_{\mathrm{fo,d}\gamma} = (6.0 \pm 0.2) \times 10^{-8}\ \mathrm{Gy/s},$$

which is three orders of magnitude lower than the average dose rate calculated for the neutrons produced with the deuteron beam, $d_{\mathrm{fo,dn}}$.

Finally, the ratio of the contributions of neutrons and gammas to the average dose rate in the gate oxides was evaluated for each beam in order to compare both situations and decide the best scenario. For the 18 MeV proton beam case such ratio is $d_{\mathrm{fo,pn}}/d_{\mathrm{fo,p}\gamma} = (1.2 \pm 0.2) \times 10^{3}$, whereas for the 9 MeV deuteron beam is $d_{\mathrm{fo,dn}}/d_{\mathrm{fo,d}\gamma} = (7.0 \pm 0.7) \times 10^{2}$. Hence, these results lead to the conclusion that the 18 MeV proton beam is able to provide a neutron source with a lower contribution of parasitic gammas.

## VI. Comparative with Co-60 Source

In order to assess the energy deposited in the flip-flop by the neutron source we have simulated the irradiation of this circuit by a Co-60 source. The Co-60 spectrum was introduced as an extra option in the *Primary Generator Action* class of the GEANT4 application which simulates the irradiation of the flip-flop.[32] The primary generator reproduced the irradiation field emitted by a Co-60 irradiator, model 484C, supplied by J. L. Shepperd & Assoc. The dose rate ranges from 0.001 rad(Si)/s to 500 rad(Si)/s with a 12 000 Ci $^{60}$Co source. Further, the irradiator produces a uniform field of up to 30×30 cm$^2$. The primary generator created gammas according to the energies and strengths of the main lines of the spectrum, at 1.173 MeV (line intensity of 99.974%) and 1.332 MeV (line intensity of 99.986%). Due to the extremely small solid angle subtended by the flip-flop at a distance of 1 m ($\sim 10^{-9}$ sr), the probability of having a coincidence of both gammas in the flip-flop is negligible; therefore, only one gamma was created in each event of the simulation. Further, the incidence of the gammas was perpendicular to the flip-flop, given the uniformity of the radiation field and the distance between the irradiator and the flip-flop.

The number of events simulated was also $3 \times 10^{9}$. As in the previous section, an "event" is a gamma incident on the upper surface of the flip-flop. The energy deposition rate per unit volume in the gate oxide of each transistor is represented in **Fig. 12**, assuming that the experimental dose rate is 1 rad(Si)/s. Statistical uncertainties, represented by error bars, are between 17% and 50% (1 $\sigma$). The value of the energy deposition rate per unit volume is between 50 eV $\mu$m$^{-3}$ s$^{-1}$ and 250 eV $\mu$m$^{-3}$ s$^{-1}$. For comparison purposes with the results shown in Section V, the average dose rate in the field oxides, $d_{\mathrm{fo,Co\text{-}60}}$, produced by a 1 rad(Si)/s Co-60 source, was also calculated. Its estimated value was

$$d_{\mathrm{fo,Co\text{-}60}} = (8.1 \pm 0.2) \times 10^{-3}\ \mathrm{Gy/s},$$

which is 4-5 orders of magnitude bigger than the previously calculated dose rate for gammas emitted from the $^{9}$Be source. Therefore, a low dose rate setup is a good scenario to compare with the situations discussed in Section V.

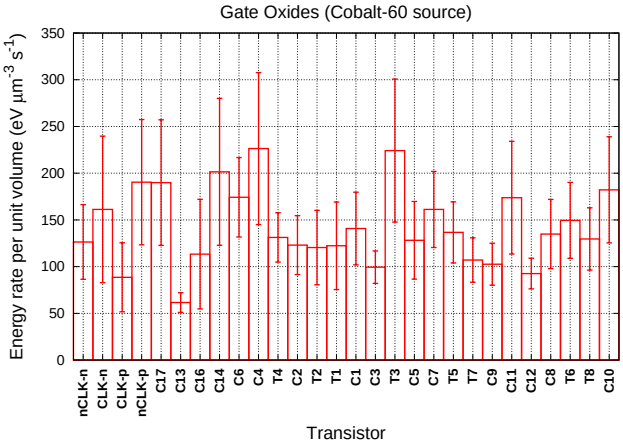


**Fig. 12** Energy deposition rate, per unit volume, by gammas emitted from a Co-60 source in the gate oxides of the flip-flop transistors. An experimental dose rate of 1 rad(Si)/s has been assumed. Labelling is the same as in Fig. 8.

## VII. Conclusions

A new neutron source designed at CNA facility (Seville, Spain) has been simulated with the GEANT4 toolkit. Specifically, the spectral yields of secondaries emitted from this source (composed of a $^{9}$Be slab and a refrigerator drum) was simulated. For the production of neutrons we have considered experimental data, whereas for the gamma production we relied on GEANT4, since no experimental data were available. At this point it is worth to mention that the spurious peaks in the emission spectra of gammas at $0^{o}$ come from a reported dysfunction of *G4NeutronHPInelastic process*, at present under an intense development work which will fix that issue (among others in low energy neutron transport) in next GEANT4 releases. In any case, the spurious gamma yields are very similar in both cases, whereas the total gamma production is higher with the deuteron beam which leads to the conclusion that the proton beam will produce a neutron source of higher quality (less gamma contamination). For the moment, these simulations have been useful for preliminary designs of this new neutron source in order to arrange a suitable setup.

Monte Carlo microdosimetry simulations of a realistic flip-flop under neutron and gamma irradiation have been presented in this work as well. A GEANT4 application to calculate the energy deposition in key elements of a flip-flop in different cases was developed. In particular, the irradiation with a standard Co-60 source was simulated as well as the irradiation with neutrons and gammas coming from the new neutron source described in this work. These calculations will be very useful to assess radiation damage of the real flip-flop under different radiation fields in several future experiments with the IBA cyclotron and the Shepperd gamma source at CNA, Sevilla, Spain.

## Acknowledgments

We would like to thank Dr. Tatsumi Koi (Stanford Linear Accelerator Center [SLAC], USA) for his kind help with GEANT4 neutron HP library.

This work was supported by Junta de Andalucía and the Spanish Ministerio de Ciencia e Innovación Contracts P07-FQM-02894, FIS2008-04189 and FPA2008-04972-C03.

## References

1) S. Agostinelli, J. Allison, K. Amako *et al.*, "GEANT4-A simulation toolkit," *Nucl. Instr. Meth. Phys. Res.*, **A506**, 250-303 (2003).
2) CNA website, http://intra.sav.us.es:8080/cna/
3) D. A. Prokopovich, M. I. Reinhard, I. M. Cornelius, A. B. Rosenfeld, "GEANT4 simulation of the CERN-EU high energy Reference Field (CERF) facility," *Radiat. Prot. Dosim.*, **141**[2], 106-113 (2010).
4) J. García López, I. Ortega-Feliu, Y. Morilla, A. Ferrero, "The new Cyclone 18/9 beam transport line at the CNA (Sevilla) for high energy PIXE applications," *Nucl. Instr. Meth. Phys. Res.*, **B266**, 1583-1586 (2008).
5) K. Yajima, H. Yasuda, M. Takada, T. Sato, T. Goka, H. Matsumuto, T. Nakamura, "Measurements of Cosmic-Ray neutron energy spectra from thermal to 15 MeV with bonner ball neutron detector in aircraft," *J. Nucl. Sci. Technol.*, **47**[1], 31-39 (2010).
6) Website of MOSIS, http://www.mosis.com
7) Website of FASTRAD software, http://www.fastrad.net
8) R. Chytracek, J. McCormic, W. Pokorski, G. Santin, "Geometry description markup language for physics simulation and analysis applications," *IEEE Trans. Nucl. Sci.*, **53**[5], 2892-2896 (2006).
9) T. N. Massey, D. K. Jacobs, S. I. Al-Quraishi, S. M. Grimes, C. E. Brient, W. B. Howard, J. C. Yanch, "Study of the Be(p,n) and Be(d,n) source reactions," *J. Nucl. Sci. Technol.*, **Supp. 2**, 677-680 (2002).
10) T. Takata, H. Tanaka, Y. Sakurai, A. Maruhashi, "Increase in irradiation beam intensity using a hybrid target system in cyclotron-based neutron capture therapy," *J. Nucl. Sci. Technol.*, **47**[7], 575-581 (2010).
11) W. Chang, "A Framework for Understanding Fast-Neutron Induced Defects in SiO2 MOS Structures," *J. Electron. Mater.*, **21**, 693-699 (1992).
12) G. P. Summers, E. A. Burke, P. Shapiro, S. R. Messenger, R. J. Walters, "Damage Correlations in Semiconductors Exposed to Gamma, Electron and Proton Radiations," *IEEE Trans. Nucl. Sci.*, **40**[6], 1372-1379 (1993).
13) G. P. Summers, E. A. Burke, M. A. Xapsos, "Displacement Damage Analog to Ionizion Radiation Effects," *Radiat. Meas.*, **24**[1], 1-8 (1995).
14) H. J. Brede, G. Dietze, K. Kudo, U. J. Schrewe, F. Tancu, C. Wen, "Neutron Yields from Thick Be Targets Bombarded with Deuterons or Protons," *Nucl. Instr. Meth. Phys. Res.*, **A274**, 332-344 (1989).
15) R. Eckhardt, "The beginning of the Monte Carlo method," *Los Alamos Science (1987 Special Issue dedicated to Stanislaw Ulam)*, 125-130 (1987).
16) S. Garny, G. Leuthold, V. Mares, H. G. Paretzke, W. Rühm, "GEANT4 Transport Calculations for Neutrons and Photons Below 15 MeV," *IEEE Trans. Nucl. Sci.*, **56**[4], 2392-2396 (2009).
17) R. Lemrani, M. Robinson, V. A. Kudryavtsev, M. De Jesus, G. Gerbiera, N. J. C. Spooner, "Low-energy neutron propagation in MCNPX and GEANT4," *Nucl. Instr. Meth. Phys. Res.*, **A560**, 454-459 (2006).

18) N. Patronis, M. Kokkoris, D. Giantsoudi, G. Perdikakis, C. T. Papadopoulos, R. Vlastou, "Aspects of GEANT4 Monte-Carlo calculations of the BC501A neutron detector," *Nucl. Instr. Meth. Phys. Res.*, **A578**, 351-355 (2007).

19) P. Sauvan, J. Sanz, F. Ogando, "New capabilities for Monte Carlo simulation of deuteron transport and secondary products generation," *Nucl. Instr. Meth. Phys. Res.*, **A614**, 323-330 (2010).

20) Website of the IAEAphsp code, http://www-nds.iaea.org/phsp/Geant4

21) S. Chauvie, S. Guatelli, V. Ivanchenko, F. Longo, F. Mantero, B. Mascialino, P. Nieminen, L. Pandola, S. Parlati, L. Peralta, M. G. Pia, M. Piergentili, P. Rodrigues, S. Saliceti, A. Trindale, "GEANT4 low energy electromagnetic physics," *Proc. Int. Conf. on Computing in High Energy and Nuclear Physics, CHEP2001*, Beijing, China, September 3-7, 2001 (2001).

22) S. Chauvie, S. Guatelli, V. Ivanchenko, F. Longo, F. Mantero, B. Mascialino, P. Nieminen, L. Pandola, S. Parlati, L. Peralta, M. G. Pia, M. Piergentili, P. Rodrigues, S. Saliceti, A. Trindale, "Geant4 Low Energy Electromagnetic Physics," *IEEE Nucl. Sci. Symp. 2004 Conf. Rec.*, **3**, 1881-1885, 2004.

23) Geant4 Reference Physics Lists website, http://geant4.web.cern.ch/support/proc_mod_catalog/physics_lists/referencePL.shtml

24) D. E. Cullen, J. H. Hubbell, L. Kissel, *EPDL97: the Evaluated Photon Data Library, '97 version*, UCRL-50400, vol. 6, rev. 5, Lawrence Livermore National Laboratory (LLNL) (1991).

25) S. T. Perkins, D. E. Cullen, S. M. Seltzer, *Tables and Graphs of Electron-Interaction Cross-Sections from 10 eV to 100 GeV Derived from the LLNL Evaluated Electron Data Library (EEDL), Z=1-100*, UCRL-50400, vol. 31, Lawrence Livermore National Laboratory (LLNL) (1991).

26) S. T. Perkins, D. E. Cullen, M. H. Chen, J. H. Hubbell, J. Rathkopf, J. Scofield, *Tables and Graphs of Atomic Subshell and Relaxation Data Derived from the LLNL Evaluated Atomic Data Library (EADL), Z=1-100*, UCRL-50400, vol. 30, Lawrence Livermore National Laboratory (LLNL) (1991).

27) H. Burkhardt, V. M. Grichine, V. N. Ivanchenko, P. Gumplinger, R. P. Kokoulin, M. Maire, L. Urban, "Geant4 'standard' electromagnetic physics package," *Proc. MC2005*, Chattanooga, Tennessee, April 17-21, 2005, American Nuclear Society, LaGrange Park, II (2005), [CD-ROM].

28) GEANT4 User's Guide for Application Developers (chapter 5), http://geant4.web.cern.ch/geant4/UserDocumentation/UsersGuides/ForApplicationDeveloper/html/ch05s04.html

29) http://www.nndc.bnl.gov/exfor/endf00.jsp

30) http://www.nea.fr/dbdata/projects/nds_jef.htm

31) http://wwwndc.jaea.go.jp/jendl/jendl.html

32) M. A. Cortés-Giraldo, F. R. Palomo, E. García-Sánchez, J. M. Quesada, "GEANT4 microdosimetry study of ionizing radiation effects in digital ASIC's," *Proc. of Joint Int. Conf. on Supercomputing in Nuclear Applications and Monte Carlo 2010 (SNA+MC2010)*, Tokyo, Japan, October 17-21, 2010 (2010).

33) F. R. Palomo, J. M. Mogollón, J. Nápoles, H. Guzmán-Miranda, A. P. Vega-Leal, M. A. Aguirre, P. Moreno, C. Méndez, J. R. Vázquez de Aldana, "Pulsed Laser SEU Cross Section Measurement Using Coincidence Detectors," *IEEE Trans. Nucl. Sci.*, **56**[4], 2001-2007 (2009).

34) B. R. B. Walters, I. Kawrakow, D. W. O. Rogers, "History by history statistical estimators in the BEAM code system," *Med. Phys.*, **29**, 2745-2752 (2002).